Two-dimensional electron liquid state at $LaAlO_3$-$SrTiO_3$ interfaces

M. Breitschaft,[1] V. Tinkl,[1] N. Pavlenko,[1,2] S. Paetel,[1] C. Richter,[1] J. R. Kirtley,[1] Y. C. Liao,[1] G. Hammerl,[1] V. Eyert,[1] T. Kopp,[1] and J. Mannhart[1,*]

[1]*Center for Electronic Correlations and Magnetism, University of Augsburg, D-86135 Augsburg, Germany*

[2]*Institute for Condensed Matter Physics, 1 Svientsitsky Str., UA-79011 Lviv, Ukraine*

(Received 28 January 2010; revised manuscript received 11 March 2010; published 30 April 2010)

Using tunneling spectroscopy we have measured the spectral density of states of the mobile, two-dimensional electron system generated at the $LaAlO_3$-$SrTiO_3$ interface. As shown by the density of states the interface electron system differs qualitatively, first, from the electron systems of the materials defining the interface and, second, from the two-dimensional electron gases formed at interfaces between conventional semiconductors.

DOI: 10.1103/PhysRevB.81.153414 PACS number(s): 73.20.−r, 73.40.Gk, 71.15.Mb

Two-dimensional (2D) conducting electron systems are generated at interfaces between a large variety of insulating oxides.[1,2] These interfaces show a broad spectrum of different properties. The quantum-Hall effect has been found,[3] for example, for the electron system at the ZnO-($Mg_xZn_{1-x}O$) interface. For the interface between $LaTiO_3$ and $SrTiO_3$, first explored experimentally by Ohtomo and Hwang,[4] spin ordering and ferro-orbital ordering has been predicted.[5] The most widely investigated electron system at oxide interfaces is the metallic state created at the interface between the charge transfer insulators $LaAlO_3$ and TiO_2-terminated $SrTiO_3$.[1] This electron system forms a 2D superconductor with a T_c of $\approx$250 mK that is easily tunable by electric gate fields.[6] The $LaAlO_3$-$SrTiO_3$ interface has also been predicted[7] and reported[8] to develop magnetic order.

While several theoretical models have been developed to describe the electronic properties of these interfaces,[9–12] less information on the electronic structure has been provided by experiments. At room temperature its thickness has been inferred from scanning tunneling microscopy (STM) writing experiments,[13] from photoemission,[14] and from cross-sectional STM (Ref. 15) to be at most a few nanometers. Further, hard x-ray photoelectron emission has shown that the charge carriers at the interface occupy Ti 3*d* states.[14] Studies of x-ray absorption spectroscopy furthermore revealed that energetically the crystal-field split Ti levels are rearranged, such that the $3d_{xy}$ levels are the first available states for the conducting electrons.[16]

The spectral density of states (DOS) at the interface is a fundamental property that characterizes the electron system. As it furthermore can be calculated as well as measured, it is a key property for the understanding of the electron system at the interface. For measurements of the spectral DOS scanning tunneling spectroscopy (STS) is a powerful technique,[17] which has been used extensively to characterize 2D electron gases (2DEGs) in semiconductor systems. STS was employed, in particular, to probe surfaces of semiconducting thin films where electrons are confined by the film thickness.[18] STS was also used successfully to analyze cross-sectional cleavage planes of semiconductor heterostructures.[19,20] In addition, semiconductor surfaces, below which electrons are confined in band bending regions induced by ion implantation[21] or surfaces at which electron gases were generated by adsorbates,[22] were explored.

Here we report on STS measurements of the spectral DOS of the electron system at the $LaAlO_3$-$SrTiO_3$ interface. We find the measured DOS to be in excellent agreement with the interface DOS calculated in density-functional theory (DFT), providing evidence that the tunneling current in the STS measurements is carried by interface states. The measured spectrum of the interface DOS and therefore the electron system differs qualitatively from the DOS of doped bulk $SrTiO_3$ or $LaAlO_3$. The electron system cannot be accurately described as a thin layer of doped $SrTiO_3$. The measurements reveal furthermore that the electron system also differs qualitatively from the hitherto known 2D electron systems at interfaces between conventional semiconductors. We find the electrons confined in multiple layers of quantum wells given by the ionic potentials of the TiO_6 octahedra. In these wells the electrons are subject to the correlations characteristic of the *d* orbitals of the Ti ions. The spectral DOS is not a step function as is the case for standard semiconductor interfaces but rather resembles the DOS of Ti 3*d* states. Quantum wells and electronic systems of this kind are unknown from the 2DEGs in conventional semiconductors, in graphene or in ZnO.

For the studies, we fabricated $LaAlO_3$-$SrTiO_3$ heterostructures with 4 unit-cell (uc) thick ($\approx$1.6 nm) epitaxial $LaAlO_3$ layers to obtain measurable tunneling currents. This thickness was chosen because it is the minimum thickness required to generate the conducting interface.[23] For larger $LaAlO_3$ thicknesses the tunneling current densities become impractically small. The samples were grown by standard pulsed laser deposition as described in Ref. 24. For deposition the $SrTiO_3$ substrates were heated to 780 °C in an oxygen background pressure of 8×10^{-5} mbar. The $LaAlO_3$ film growth was monitored by reflection high-energy electron diffraction. While $SrTiO_3$ surfaces are known to show numerous surface reconstructions,[25–32] x-ray diffraction showed no evidence of distortions of the $LaAlO_3$ films, which could be attributed to a $SrTiO_3$ surface reconstruction, suggesting that the $LaAlO_3$ growth stabilizes the standard $SrTiO_3$ structure at the interface. Titanium plugs filling ion etched holes were used to contact the interfaces. After a heating procedure in a preparation chamber,[24] the samples were transferred *in situ* to the scanning probe microscope (SPM), which operates in ultrahigh vacuum at 4.7 K. An iridium spall attached to a cantilever based on a quartz tuning fork[33] with a spring con-

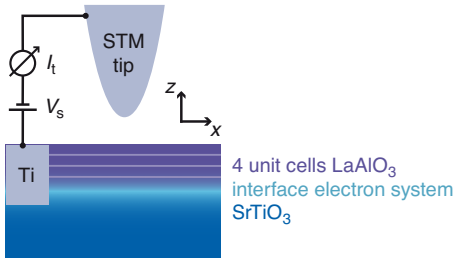

FIG. 1. (Color online) Illustration of the experimental configuration. A metallic state is formed at the interface between the $SrTiO_3$ substrate and a 4 uc thick layer of $LaAlO_3$. Scanning tunneling microscopy and spectroscopy are performed by monitoring the tunneling current I_t between the tip and the sample as a function of V_s, the voltage at the sample relative to the tip.

stant of 1800 N/m was used as a tip. The tip was treated *in situ* by field emission.[24] The cantilever was not excited mechanically during STM and STS measurements. The experimental setup is sketched in Fig. 1. Typical measurement parameters were tunneling currents of 10 pA, sweep rates of 0.01 V/s and scanning speeds of 10 nm/s.

Imaging the $LaAlO_3$-$SrTiO_3$ heterostructures by frequency modulation scanning force microscopy[34] (FM-SFM) as well as by constant current STM revealed the standard step-and-terrace structure resulting from the slight miscut of the $SrTiO_3$ substrates (Fig. 2). While on more conventional samples excellent resolution was achieved with the SPM employed,[35] it was impossible to obtain atomic resolution on the $LaAlO_3$-$SrTiO_3$ heterostructures.[24]

Conductance-voltage characteristics $\partial I_t/\partial V_s(V_s)$ were measured using a standard lock-in technique.[24] Simultaneously, the tunneling current was measured as a function of voltage. The normalized differential conductance, NDC

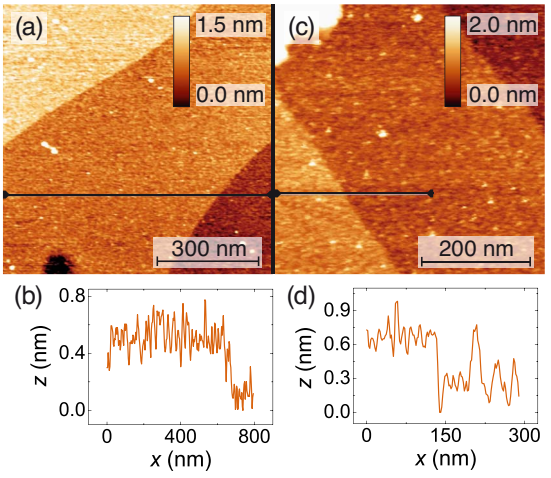

FIG. 2. (Color online) Scanning probe microscopy images of $LaAlO_3$-$SrTiO_3$ heterostructures. (a) Topographic FM-SFM image of the $LaAlO_3$ film. (b) Profile taken along the line indicated in (a). (c) Topographic STM image acquired on the $LaAlO_3$-$SrTiO_3$ heterostructure recorded with a scanning speed of 5 nm/s, a bias voltage V_s=2 V, and a current set point of 10 pA. (d) Profile taken along the line indicated in (c). All data were taken at 4.7 K. For further detail see Ref. 24.

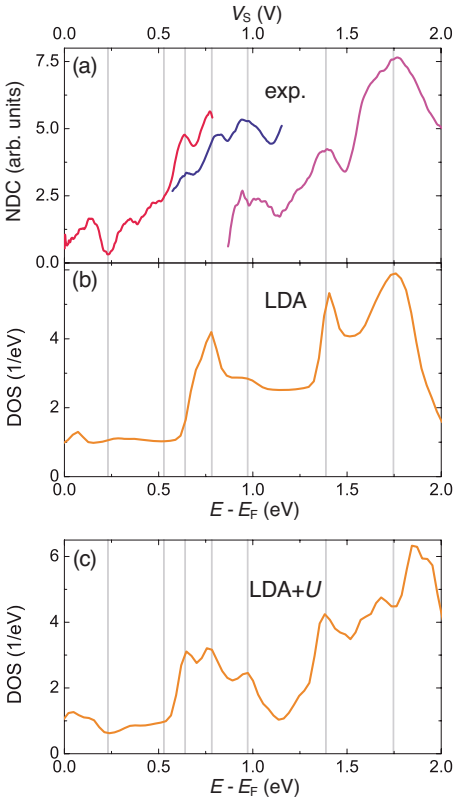

FIG. 3. (Color online) Comparison of the measured differential conductance and DFT calculated state densities. (a) NDC(V_s) $=(\partial I_t/\partial V_s)/(I_t/V_s+\epsilon)(V_s)$ characteristics with ϵ=1 pA/V measured at several sites located far away from topographic steps. The measurements were performed at 4.7 K with fixed tip-sample separations. The different colors reflect different tip-sample separations [purple (light gray): $I_{t,stab}$=70 pA, $V_{s,stab}$=2.4 V; blue (dark gray): $I_{t,stab}$=12 pA, $V_{s,stab}$=1 V; and red (medium gray): $I_{t,stab}$=12 pA, $V_{s,stab}$=0.8 V]. The data were averaged over an interval of 75 mV. The purple (light gray) characteristic was measured on a different sample than the red (medium gray), and blue (dark gray) ones. (b) Ti 3*d* DOS of the interface TiO_2 layer calculated using LDA for a supercell with a 4 uc thick $LaAlO_3$ layer. (c) Ti 3*d* DOS of the interface TiO_2 layer calculated using LDA+U. In (a)–(c) the positions of characteristic features in the NDC are marked with gray lines.

$\equiv(\partial I_t/\partial V_s)/(I_t/V_s+\epsilon)$ was determined as a measure of the sample DOS.[36] The spectra were taken on sample areas where the step-and-terrace structure was resolved in STM topography. We found the characteristic spectroscopic features to be reproducible across four samples.[24] Figure 3(a) shows a representative dependence of the NDC on voltage. The conductances are minute for negative voltages (tunneling from occupied sample states). For positive voltages (tunneling into unoccupied sample states) the spectroscopically accessible energy range is limited at low voltages by small tunneling conductances and at high voltages by large electric fields destabilizing the tunneling gap. To measure the tunneling characteristics at a given sample location over a large voltage range, several spectra were therefore taken at different tip-sample separations as determined according to the tunneling currents $I_{t,stab}$ at given gap voltages $V_{s,stab}$. Three

characteristics measured with different tip-sample separations, from two different samples, are shown in Fig. 3(a). In these spectra, clear peaks are seen at ≈0.6, ≈0.8, ≈1, ≈1.4, and ≈1.8 V.

To identify the electron states carrying the measured tunneling current and to explore the role of electronic correlations at the interface we compare the measured DOS to predictions of DFT. We performed local-density approximation (LDA) and LDA+U calculations[37,38] of the layer-resolved DOS of $LaAlO_3$-$SrTiO_3$ heterostructures. Further information on these calculations is given in Ref. 24. While differences are present in details, the calculated state densities and the effective electron mass of 3.25 bare electron masses are consistent with those reported in Refs. 9, 10, 39, and 40.

In Fig. 3(b) the Ti 3d DOS of the interface TiO_2 layer calculated using LDA for a supercell with a 4 uc thick $LaAlO_3$ layer on $SrTiO_3$ is shown. According to the calculation, electronic reconstruction leads to a doping of O 2p states located in the topmost AlO_2 layer with holes and of Ti 3d t_{2g} states located at the interface with electrons. Experimentally, it is only the interface which is found to be conducting. In the total DOS between 0 and 2 eV the Ti 3d t_{2g} orbitals located in the interfacial TiO_2 layer prevail. The other, small, contributions are provided by the TiO_2 planes of adjacent $SrTiO_3$ layers and, below ≈0.5 eV, by the O 2p states of the surface. The Ti 3d e_g states contribute at energies above ≈2.8 eV and the La 5d states at energies above ≈2.2 eV. The measured peaks at ≈0.8, ≈1.4, and ≈1.8 V are also present in the calculated DOS. The measured peaks at ≈0.6 and ≈1 V, however, are not represented in the LDA result.

The LDA+U calculations of the interface electron system consider an on-site Coulomb repulsion U=2 eV and a Hund coupling J=0.8 eV in the Ti 3d shell. The choice of conservative values for U and J does not imply these values characterize the system best. Figure 3(c) shows the DOS calculated for the supercell using LDA+U. The DOS exhibits additional peaks at ≈0.6 and ≈1 eV, generated by the splitting of the Ti $3d_{xz}$+$3d_{yz}$ bands due to the interorbital interactions caused by the finite U and J. Remarkably, these peaks are observed experimentally but are missing in the LDA DOS.

We note that the experimental hump at ≈1.8 eV is broader than the corresponding structure in LDA. However, LDA+U generates a structure of approximately the measured width but with finer structures. These fine structures reflect the formation of the upper Hubbard bands, which is a fundamental effect of correlated electron systems, arising when U is on the order of the bandwidth or larger. Indeed, the calculated width of the Ti 3d t_{2g} band is ≈2 eV=U.

The good agreement between experiment and calculation suggests that the electron states carrying the measured tunneling current are the ones calculated in DFT. For energies between 0.5 and 2 eV, mainly Ti $3d_{xz}$+$3d_{yz}$ and Ti $3d_{xy}$ orbitals of the interface TiO_2 layer contribute to the calculated DOS and the prominent peaks result from these orbitals; tunneling occurs into Ti 3d orbitals at the interface, the significant contributions arising from the Ti 3d t_{2g} states. These results are consistent with the results of recent photoabsorption measurements,[16] from which it was concluded that the lowest unoccupied states are Ti $3d_{xy}$ states.

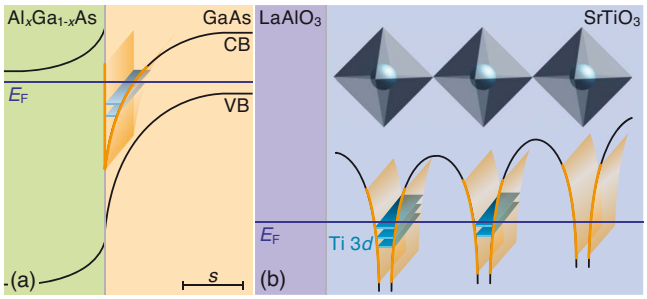

FIG. 4. (Color online) Illustration of the configuration of 2D electron systems in standard semiconductor interfaces and at the $LaAlO_3$-$SrTiO_3$ interface. (a) At the interface between the semiconductors an electron gas is generated at a potential well created by band bending, which typically has a width of tens of nanometers as determined by the electronic screening length s. The electron states can be approximated by the states of free electrons in this potential well. (b) At the oxide interface the potential well is provided by the Coulomb potential of the titanium ions in the TiO_6 octahedra and, to a smaller extent, by band bending. These potential wells are narrower than those at semiconductor interfaces; the "resonant" electron states are well approximated by the Ti 3d t_{2g} states, which form a 2D electron system extended parallel to the interface. Due to the electronic correlations of the oxide lattices, the mobile electrons form an electron liquid.

The fact that the experimental DOS is matched significantly better by the LDA+U calculation than by the LDA calculation provides evidence that the electron system at the interface is correlated with substantial values of U and J on the Ti 3d orbitals. Therefore, this 2D electron system is a liquid. This electron liquid is formed by correlated electrons, which can move parallel to the interface, but are constrained in their perpendicular motion by the Coulomb potentials of the titanium ions of the final TiO_2 layers and also, to a smaller degree, by band bending (Fig. 4).

Interfaces in oxides therefore broaden the spectrum of available 2D electron systems from the 2DEGs of conventional semiconductors to also include systems with sizable electronic correlations. Such correlation effects, in combination with the already intriguing physics of 2D electron systems, promise unprecedented electronic phenomena. Influenced by electronic correlations generated in the ionic lattices of the oxides, electron systems at oxide interfaces have exceptional properties, possibly enabling devices with hitherto unknown characteristics.

We thank D. Bonn, R. Claessen, M. Fiebig, F. J. Giessibl, J. Repp, C. W. Schneider, and D. Vollhardt for helpful discussions. This work was supported by the Deutsche Forschungsgemeinschaft (TRR 80) and by the European Union (OxIDes). J.R. Kirtley was supported by the Alexander von Humboldt foundation. Grants of computer time from the Leibniz-Rechenzentrum München through HLRB (h1181) and DEISA (OXSIM) are gratefully acknowledged.

*jochen.mannhart@physik.uni-augsburg.de

[1] A. Ohtomo and H. Y. Hwang, Nature (London) **427**, 423 (2004).
[2] J. Mannhart, D. H. A. Blank, H. Y. Hwang, A. J. Millis, and J.-M. Triscone, MRS Bull. **33**, 1027 (2008).
[3] A. Tsukazaki, A. Ohtomo, T. Kita, Y. Ohno, H. Ohno, and M. Kawasaki, Science **315**, 1388 (2007).
[4] A. Ohtomo, D. A. Muller, J. L. Grazul, and H. Y. Hwang, Nature (London) **419**, 378 (2002).
[5] S. Okamoto, A. J. Millis, and N. A. Spaldin, Phys. Rev. Lett. **97**, 056802 (2006).
[6] A. D. Caviglia, S. Gariglio, N. Reyren, D. Jaccard, T. Schneider, M. Gabay, S. Thiel, G. Hammerl, J. Mannhart, and J.-M. Triscone, Nature (London) **456**, 624 (2008).
[7] R. Pentcheva and W. E. Pickett, Phys. Rev. B **74**, 035112 (2006).
[8] A. Brinkman, M. Huijben, M. van Zalk, J. Huijben, U. Zeitler, J. C. Maan, W. G. van der Wiel, G. Rijnders, D. H. A. Blank, and H. Hilgenkamp, Nature Mater. **6**, 493 (2007).
[9] N. Pavlenko and T. Kopp, arXiv:0901.4610 (unpublished).
[10] R. Pentcheva and W. E. Pickett, Phys. Rev. Lett. **102**, 107602 (2009).
[11] U. Schwingenschlögl and C. Schuster, Chem. Phys. Lett. **467**, 354 (2009).
[12] U. Schwingenschlögl and C. Schuster, EPL **86**, 27005 (2009).
[13] C. Cen, S. Thiel, G. Hammerl, C. W. Schneider, K. E. Andersen, C. S. Hellberg, J. Mannhart, and J. Levy, Nature Mater. **7**, 298 (2008).
[14] M. Sing *et al.*, Phys. Rev. Lett. **102**, 176805 (2009).
[15] M. Basletic, J.-L. Maurice, C. Carrétéro, G. Herranz, O. Copie, M. Bibes, É. Jacquet, K. Bouzehouane, S. Fusil, and A. Barthélémy, Nature Mater. **7**, 621 (2008).
[16] M. Salluzzo *et al.*, Phys. Rev. Lett. **102**, 166804 (2009).
[17] R. M. Feenstra, Surf. Sci. **299-300**, 965 (1994).
[18] S. Perraud, K. Kanisawa, Z.-Z. Wang, and T. Fujisawa, Phys. Rev. Lett. **100**, 056806 (2008).
[19] H. W. M. Salemink, H. P. Meier, R. Ellialtioglu, J. W. Gerritsen, and P. R. M. Muralt, Appl. Phys. Lett. **54**, 1112 (1989).
[20] K. Suzuki, K. Kanisawa, C. Janer, S. Perraud, K. Takashina, T. Fujisawa, and Y. Hirayama, Phys. Rev. Lett. **98**, 136802 (2007).
[21] M. Wolovelsky, Y. Goldstein, and O. Millo, Phys. Rev. B **57**, 6274 (1998).
[22] M. Morgenstern, J. Klijn, C. Meyer, and R. Wiesendanger, Phys. Rev. Lett. **90**, 056804 (2003).
[23] S. Thiel, G. Hammerl, A. Schmehl, C. W. Schneider, and J. Mannhart, Science **313**, 1942 (2006).
[24] See supplementary material at http://link.aps.org/supplemental/10.1103/PhysRevB.81.153414 for more data and details on sample preparation, STM tip treatment, experimental parameters, the STS lock-in technique, and the DFT calculations.
[25] R. Herger, P. R. Willmott, O. Bunk, C. M. Schlepütz, B. D. Patterson, and B. Delley, Phys. Rev. Lett. **98**, 076102 (2007).
[26] C. Lu, E. Zhu, Y. Liu, Z. Liu, Y. Lu, J. He, D. Yu, Y. Tian, and B. Xu, J. Phys. Chem. C **114**, 3416 (2010).
[27] D. S. Deak, F. Silly, K. Porfyrakis, and M. R. Castell, Nanotechnology **18**, 075301 (2007).
[28] R. I. Eglitis and D. Vanderbilt, Phys. Rev. B **77**, 195408 (2008).
[29] Z. Wang, K. Wu, Q. Guo, and J. Guo, Appl. Phys. Lett. **95**, 021912 (2009).
[30] F. Silly, D. T. Newell, and M. R. Castell, Surf. Sci. **600**, 219 (2006).
[31] T. Kubo and H. Nozoye, Surf. Sci. **542**, 177 (2003).
[32] D. T. Newell, A. Harrison, F. Silly, and M. R. Castell, Phys. Rev. B **75**, 205429 (2007).
[33] F. J. Giessibl, Appl. Phys. Lett. **73**, 3956 (1998).
[34] T. R. Albrecht, P. Grütter, D. Horne, and D. Rugar, J. Appl. Phys. **69**, 668 (1991).
[35] S. Hembacher, F. J. Giessibl, and J. Mannhart, Science **305**, 380 (2004).
[36] R. M. Feenstra, J. A. Stroscio, and A. P. Fein, Surf. Sci. **181**, 295 (1987).
[37] P. Blaha, K. Schwarz, G. K. H. Madsen, D. Kvasnicka, and J. Luitz, *WIEN2k*, edited by K. Schwarz (Vienna University of Technology, Vienna, Austria, 2001).
[38] V. I. Anisimov, I. V. Solovyev, M. A. Korotin, M. T. Czyżyk, and G. A. Sawatzky, Phys. Rev. B **48**, 16929 (1993).
[39] U. Schwingenschlögl and C. Schuster, EPL **81**, 17007 (2008).
[40] O. Copie *et al.*, Phys. Rev. Lett. **102**, 216804 (2009).